www.nature.com/npp

American College of Neuropsychopharmacology

ARTICLE

Check for updates

Brain-based graph-theoretical predictive modeling to map the trajectory of anhedonia, impulsivity, and hypomania from the human functional connectome

Rotem Dan[1,2], Alexis E. Whitton[1,2,3], Michael T. Treadway[4,5], Ashleigh V. Rutherford[1], Poornima Kumar[1,2], Manon L. Ironside[1], Roselinde H. Kaiser[6], Boyu Ren[2,7] and Diego A. Pizzagalli[1,2]✉

Clinical assessments often fail to discriminate between unipolar and bipolar depression and identify individuals who will develop future (hypo)manic episodes. To address this challenge, we developed a brain-based graph-theoretical predictive model (GPM) to prospectively map symptoms of anhedonia, impulsivity, and (hypo)mania. Individuals seeking treatment for mood disorders ($n = 80$) underwent an fMRI scan, including (i) resting-state and (ii) a reinforcement-learning (RL) task. Symptoms were assessed at baseline as well as at 3- and 6-month follow-ups. A whole-brain functional connectome was computed for each fMRI task, and the GPM was applied for symptom prediction using cross-validation. Prediction performance was evaluated by comparing the GPM to a corresponding null model. In addition, the GPM was compared to the connectome-based predictive modeling (CPM). Cross-sectionally, the GPM predicted anhedonia from the global efficiency (a graph theory metric that quantifies information transfer across the connectome) during the RL task, and impulsivity from the centrality (a metric that captures the importance of a region) of the left anterior cingulate cortex during resting-state. At 6-month follow-up, the GPM predicted (hypo)manic symptoms from the local efficiency of the left nucleus accumbens during the RL task and anhedonia from the centrality of the left caudate during resting-state. Notably, the GPM outperformed the CPM, and GPM derived from individuals with unipolar disorders predicted anhedonia and impulsivity symptoms for individuals with bipolar disorders. Importantly, the generalizability of cross-sectional models was demonstrated in an external validation sample. Taken together, across DSM mood diagnoses, efficiency and centrality of the reward circuit predicted symptoms of anhedonia, impulsivity, and (hypo)mania, cross-sectionally and prospectively. The GPM is an innovative modeling approach that may ultimately inform clinical prediction at the individual level.

Neuropsychopharmacology (2024) 49:1162–1170; https://doi.org/10.1038/s41386-024-01842-1

INTRODUCTION

A major challenge in the treatment of mood disorders is to distinguish between unipolar and bipolar depression and, specifically, to predict future bipolar symptoms. Current assessments often fail to recognize the risk of developing manic symptoms in individuals seeking treatment during a depressive episode [1, 2]. It has been documented that up to 25% of individuals with major depressive disorder (MDD) might actually have an undiagnosed bipolar disorder (BD) [3], with rates reaching 50% in treatment-resistant depression [4]. This misdiagnosis can be dangerous, as standard pharmacotherapy (i.e., SSRIs) for unipolar depression can trigger or exacerbate manic symptoms [5]. Given that manic episodes can result in devastating financial, legal, and professional consequences as well as poor prognosis [1], there is a crucial need to identify pathophysiological mechanisms that predict the development of bipolar symptoms.

Predictive modeling, i.e., data-driven machine-learning models, can provide a powerful approach for predicting clinical symptoms at the individual level. The major advantage of predictive modeling over standard correlational/regression analyses is that they utilize cross-validation, where the model is built on a subsample of the data (training set), and prediction is done on a separate subsample (testing set). This method is crucial for increasing generalizability and reducing overfitting [6]. For psychiatric research especially, the generalization of findings to unseen patients is essential for clinical translation, e.g., for developing robust biomarkers. Brain-based biomarkers can be tailored based on circuit-level functional measures and used as targets for therapeutic interventions, including transcranial magnetic stimulation and neurofeedback [7, 8].

The connectome-based predictive modeling (CPM) [9] is a cross-validation model that maps phenotype measures (e.g., behavior, cognition) to whole-brain patterns of functional connections (hereafter "functional connectomes"). The CPM utilizes a unique method for feature selection, where the functional connections that are most strongly correlated with

[1]Center for Depression, Anxiety and Stress Research, McLean Hospital, Belmont, MA, USA. [2]Department of Psychiatry, Harvard Medical School, Boston, MA, USA. [3]Black Dog Institute, University of New South Wales, Sydney, Australia. [4]Department of Psychology, Emory University, Atlanta, GA, USA. [5]Department of Psychiatry and Behavioral Sciences, Emory University, Atlanta, GA, USA. [6]Department of Psychology and Neuroscience, University of Colorado Boulder, Boulder, CO, USA. [7]Laboratory for Psychiatric Biostatistics, McLean Hospital, Belmont, MA, USA. ✉email: dap@mclean.harvard.edu

Received: 20 October 2023 Revised: 27 January 2024 Accepted: 1 March 2024
Published online: 13 March 2024

the phenotype are summed together to one brain metric. The CPM was primarily used in healthy populations [10–12] but has been increasingly shown to successfully model clinical conditions, including autism [13], childhood aggression [14], and cocaine abstinence [15].

Here, we propose a new brain-based predictive modeling approach and apply it to prospectively predict the trajectory of symptoms of anhedonia, impulsivity, and (hypo)mania among treatment-seeking patients with mood disorders. By employing graph theory to define brain predictors, our brain-based graph-theoretical predictive modeling (GPM) critically extends the CPM. Graph theory is a mathematical framework that enables characterization of complex networks (here, the organization of the brain) by quantifying both integrative processes and local specialization of communities (here, of brain regions) [16]. Notably, graph-theoretical metrics have been shown to track key clinical features of mood disorders, including depression severity [17, 18], rumination [19], suicidal ideation [20], and treatment response [21, 22]. Furthermore, graph-theoretical metrics have been found to differentiate between depressed individuals with BD and MDD [23, 24]. However, to date, most prior research adopted a classification approach and did not attempt to predict symptom development in individuals.

The rationale for developing the GPM comes from the observation that complex network measures, which are derived using theoretically-based mathematical definitions, inherently encompass summations of connections [25]. For example, global efficiency is a fundamental graph-theoretical metric that captures the level of integration across the network and is based on a summation of distances between regions. By using graph-theoretical metrics as brain predictors, the feature selection step of the CPM (which sums connections) can be replaced with a theoretically driven and biologically meaningful summation of functional connections. Importantly, the specific graph-theoretical metric which is identified to have predictive utility from a diverse set of possible measures can further inform the type of brain network dysfunction that is associated with a given symptom.

Our study goals included the following. First, using the GPM, we aimed to predict reward-related symptoms in individuals with mood disorders, cross-sectionally and prospectively, from baseline neuroimaging functional connectomes. Our a priori focus was on transdiagnostic symptoms of anhedonia, impulsivity, and (hypo)mania. Notably, most neuroimaging predictive studies are cross-sectional, where symptoms and neuroimaging data are both collected at baseline. However, to have clinical utility, it is essential for a model to be able to predict the development of future symptoms (while accounting for baseline). To address this gap, a longitudinal clinical evaluation was conducted.

Second, in light of the difficulty to separate between unipolar and bipolar depression, we utilized a Research Domain Criteria (RDoC) [26] approach. In the RDoC framework, psychiatric illness is conceptualized as a continuum across behavioral, psychological, and biological measurements. Thus, DSM diagnoses were not considered in our predictive models and treatment-seeking individuals were enrolled based on their performance on a reward-learning task, to allow high variability in reward-related phenotypes. Third, we aimed to examine the influence of the cognitive state on symptom prediction. Since it has been suggested that functional connectomes acquired during tasks can improve prediction performance [27], we hypothesized that a reinforcement-learning (RL) task would increase the success of predicting reward-related symptoms. Last, we hypothesized that network measures of the reward circuit would better predict reward-related symptoms compared to whole-brain global measures.

MATERIALS AND METHODS

Participants

A sample of 80 individuals with mood disorders was recruited. The sample included 58 individuals with unipolar mood pathology (MDD, dysthymia, MDD in partial remission) and 22 individuals with bipolar mood pathology (BD type I or II, depressed, mixed, or hypomanic). Participants were treatment-seeking, although none were acutely manic or suicidal. A demographically matched sample of 32 healthy controls was also recruited to this study but were not included in analyses in light of the study's goal of modeling and predicting symptoms among treatment-seeking patients. Participants were enrolled according to their reward-learning performance as characterized by the probabilistic reward task [28], such that each quantile of the normative distribution of reward-learning was equally represented (see [29] for details). Clinical diagnoses and eligibility were evaluated using the Structured Clinical Interview for DSM-IV [30] (Supplementary Methods). Stable antidepressants or mood stabilizing medication were allowed. The study was approved by the Partners Human Research Committee and participants provided written informed consent.

Study design and evaluation of reward-related symptoms

Participants underwent an fMRI scan, including (i) resting-state and (ii) an RL task [31]. The RL dataset was previously presented [29, 32], however, resting-state datasets were not analyzed or published before. Symptoms of anhedonia, impulsivity, and (hypo)mania were measured at baseline in a separate visit before the fMRI scan and at 3- and 6-month follow-ups. Anhedonia was assessed using the Anhedonic Depression subscale of the 62-item Mood and Anxiety Symptom Questionnaire (MASQ-AD) [33], impulsivity was assessed using the Barratt Impulsiveness Scale (BIS) [34], and (hypo)mania was assessed using the Mania subscale of the Bipolar Inventory of Symptoms Scale (BISS-mania) [35].

MRI data acquisition and preprocessing

MRI data were collected at McLean Imaging Center on a 3 T Siemens Tim Trio using a 32-channel head coil. Preprocessing of fMRI data was done using fMRIPrep [36] and CONN [37] (Supplementary Methods).

Whole-brain functional connectomes

A whole-brain functional connectome was computed for each individual and paradigm (RL task, rest). Note that the three runs of the RL task were conjugated to compute one connectome. The cortex was parcellated using the Schaefer 200-node atlas [38] and the subcortex was parcellated using the Harvard-Oxford (HO) atlas [39]. Pearson's correlations were computed between the average BOLD time series from all pairs of nodes and Fisher's transforms were applied.

Graph-theoretical analysis

Graph theoretical analyses were carried out on the weighted positive functional connectome matrices using the Brain Connectivity Toolbox [25]. Negative functional connections were not included since most graph measures can be calculated only for positive weights. For each individual and state, global measures were computed across the entire network, in addition to local measures which were calculated for each of the reward circuit's regions: anterior cingulate cortex (ACC), caudate, putamen, nucleus accumbens (NAc), lateral and medial orbitofrontal cortex (OFC). (i) *Global measures:* characteristic path length, global efficiency, mean clustering coefficient, mean local efficiency, mean betweenness centrality. (ii) *Local measures:* clustering coefficient, local efficiency, betweenness centrality (Supplementary Methods).

Brain-based graph-theoretical predictive modeling (GPM)

The GPM is illustrated in Fig. 1 and includes the following steps for symptom prediction: (i) calculation of whole-brain functional connectomes; (ii) computation of graph-theoretical metrics from functional connectomes (measures of integration, segregation, centrality); (iii) feature selection: choosing the graph metric (only one) which is most strongly associated with the clinical symptom. Note that this can be either a global metric, e.g., global efficiency, or a metric of a specific region, e.g., centrality of the left caudate; (iv) model building: mapping between graph metric and clinical symptom; (v) model prediction: applying the model to previously unseen data. The GPM utilized leave-one-out cross-validation (LOOCV). In LOOCV, the data are divided in each iteration into a training set (N-1 subjects,

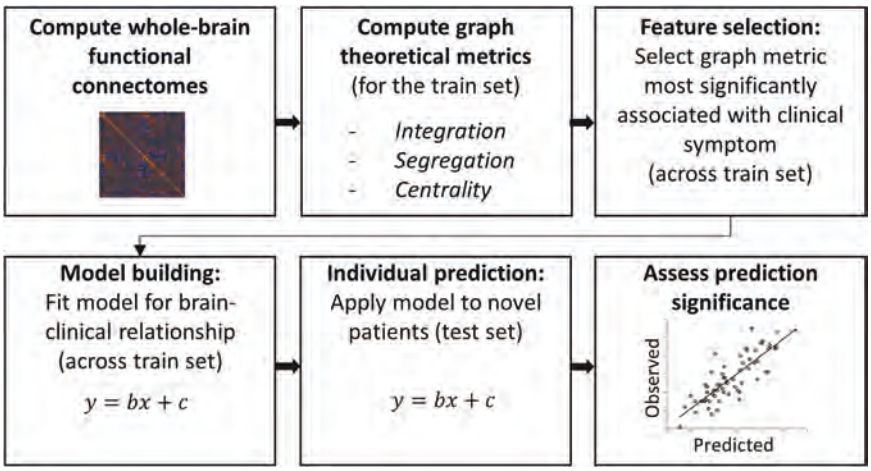

Fig. 1 Illustration of the brain-based graph-theoretical predictive modeling (GPM). The GPM utilizes cross-validation and includes the following steps: (i) calculation of whole-brain functional connectomes for each individual; (ii) computation of graph-theoretical metrics from brain connectomes; (iii) feature selection: choosing the graph metric most strongly associated with the clinical symptom; (iv) model building: mapping between graph metric and clinical symptom; (v) model prediction: applying the model to previously unseen data. The model is built on the training set (steps i-iv) and prediction is done on the testing set (step v).

where N is the sample size) and a testing set (remaining subject). The model is built on the training set (steps i-iv) and prediction is done on the testing set (step v). This procedure is repeated N times to obtain a predicted score for all participants. Note that similar results were obtained with 10-fold cross-validation (Supplementary Results).

Model building was accomplished using multiple regression while controlling for all other baseline symptoms and psychotropic medication load [40]. For example, when predicting anhedonia at baseline, (hypo) mania and impulsivity at baseline were covaried. For predicting symptom severity at follow-up, symptom severity (for all symptom scales) at baseline was covaried. For the prediction of (hypo)manic symptoms, due to the skewed distribution of scores, a log $(x+1)$ transform was used. DSM categories (MDD, BP) were not considered in the model.

The model's predictive performance (the correspondence between predicted and observed scores) was evaluated by the mean squared error (MSE) and compared to a null model. The null model was defined as the same model without the graph-theoretical brain predictor, including only baseline symptoms and psychotropic medication load. To formally compare models, the corrected repeated k-fold cv test was used [41]. Pearson's correlation was computed, and p values were obtained using permutation testing with 10,000 repetitions (Supplementary Methods).

The GPM's feature-selection step implements a "winner-take-all" approach, i.e., only the best graph-theoretical metric is included in the predictive model. As an alternative approach, we tested the inclusion of several graph-theoretical metrics by utilizing an elastic-net algorithm to generate the predictive model [42, 43] (Supplementary Methods). Finally, to further evaluate if predictions are transdiagnostic and not driven by one patient group over the other, we split the sample to unipolar and bipolar disorders, trained the GPM on the unipolar disorders group and tested on the bipolar disorders group. Due to smaller sample sizes for follow-ups, this analysis was conducted for baseline symptoms.

External validation analysis

The generalizability of our models was tested on an independent sample of 96 individuals (ages: 18-48; 77 female), including 44 MDD and 52 HC [44, 45]. Impulsivity scores were available for a subset of 53 individuals (25 MDD, 28 HC). Models were built on the primary sample and prediction was tested on the external sample. Note that for this sample, data were collected during the Monetary Incentive Delay task (MID) [46] instead of the RL task [31]. Thus, for anhedonia, the model was built on the RL task and prediction was tested on the MID. Anhedonia was predicted for individuals with MDD and impulsivity was predicted across MDD and HC. Full details are provided in the Supplementary Methods.

Comparison with the CPM

The CPM was applied for symptom prediction using available code [47]. The CPM was run on the functional connectome including negative weights, as originally done [9], and on the positive-only connectome. A threshold of $p = 0.01$ was applied for edge selection. Apart from inherent differences between the GPM and CPM, all methodological choices were kept identical (Supplementary Methods).

RESULTS

Clinical characteristics and symptom trajectories

The clinical and demographic characteristics of the sample are presented in Table 1. Eight and 13 participants, respectively, were lost to follow-up at 3- and 6-month. BIS scores at baseline were missing from 6 participants. In addition, BISS-mania scores at 3- and 6-month were missing from 1 participant; BIS and MASQ-AD scores were missing from 1 participant at 3-month follow-up and from 2 participants at 6-month follow-up. The distributions of anhedonia, impulsivity, and (hypo)mania symptoms across baseline, 3- and 6-month follow-ups are shown in Fig. 2. Supplementary Table 1 includes the list of medications used by participants and Supplementary Table 2 presents the cross-correlations among symptoms over time.

GPM symptom prediction at baseline

At baseline, the GPM predicted anhedonia from the global efficiency of the functional connectome during the RL task (Fig. 3A) [$N = 61$; GPM: $r = 0.317$, $p = 0.028$ permutation testing, MSE = 152.60; null model: $r = 0.070$, $p = 0.161$ permutation testing, MSE = 172.15]. Decreased global efficiency was associated with greater anhedonia. The GPM outperformed the null model ($t = 4.02$, $p < 10^{-4}$ corrected repeated k-fold CV test) and had an 11.35% lower MSE relative to the null model.

The GPM predicted impulsivity from the centrality of the left ACC during resting-state (Fig. 3B) [$N = 73$; GPM: $r = 0.310$, $p = 0.020$ permutation testing, MSE = 119.52; null model: $r = 0.025$, $p = 0.226$ permutation testing, MSE = 136.78]. Increased ACC centrality was associated with greater impulsivity. The GPM outperformed the null model ($t = 5.03$, $p < 10^{-4}$ corrected repeated k-fold CV test) and had a 12.62% lower MSE relative to the null model. In a post-hoc analysis, we tested whether specific subtypes of impulsivity (as measured by the six subscales of the BIS, using a Bonferroni corrected threshold of $p < 0.008$) could be predicted from the centrality of the left ACC. The GPM predicted the non-planning/self-control subscale of the BIS [$N = 73$; GPM: $r = 0.406$, $p = 3{\cdot}10^{-4}$ permutation testing, MSE = 11.72; null model: $r = 0.170$, $p = 0.052$ permutation testing, MSE = 13.82]. The GPM outperformed the null model ($t = 25.30$, $p < 10^{-4}$

Table 1. Clinical and demographic characteristics of the sample.

	Unipolar disorders ($n = 58$)	Bipolar disorders ($n = 22$)
Demographics		
Age, years, mean ± SD (range)	28.0 ± 8.6 (18-60)	31.7 ± 13.2 (18-57)
Female, *n* (%)	41 (71.7)	12 (54.5)
Education, years, mean ± SD (range)	16.0 ± 2.8 (10-25)	16.0 ± 3.0 (10-24)
White, *n* (%)	40 (69.0)	19 (86.4)
Hispanic, *n* (%)	6 (10.3)	1 (4.5)
Clinical diagnoses, *n* (%)		
Current MDD	49 (84.5)	–
Current dysthymia	1 (1.7)	–
MDD in partial remission	8 (13.8)	–
BD-I depressed	–	7 (31.8)
BD-I mixed	–	0 (0.0)
BD-I hypomanic	–	2 (9.1)
BD-II depressed	–	9 (40.9)
BD-II mixed	–	1 (4.6)
BD-II hypomanic	–	3 (13.6)
Medication, *n* (%)		
Antidepressants	19 (32.8)	3 (13.6)
Mood stabilizers or anticonvulsants	1 (1.7)	9 (40.9)
Reward-related symptoms, mean ± SD (range)		
Anhedonia (MASQ-AD)		
Baseline	81.5 ± 11.9 (49–101)	74.3 ± 12.9 (39–98)
3-month follow-up	76.1 ± 16.0 (37–102)	65.3 ± 14.7 (29–87)
6-month follow-up	73.1 ± 14.1 (38–104)	64.4 ± 14.5 (39–90)
Impulsivity (BIS)		
Baseline	67.5 ± 10.6 (45–90)	68.0 ± 13.2 (44–94)
3-month follow-up	67.7 ± 11.5 (48–93)	69.3 ± 14.8 (41–95)
6-month follow-up	67.2 ± 11.7 (44–93)	66.9 ± 13.7 (46–91)
Mania (BISS-mania)		
Baseline	5.1 ± 3.9 (0–19)	13.6 ± 10.1 (0–37)
3-month follow-up	4.5 ± 3.8 (0–18)	6.8 ± 9.6 (0–38)
6-month follow-up	3.7 ± 3.5 (0–16)	7.9 ± 11.2 (0–40)

BD-I/II bipolar disorder type I/II, *BIS* Barratt Impulsiveness Scale, *BISS-mania* Bipolar Inventory of Symptoms Scale Mania subscale, *MASQ-AD* Anhedonic Depression subscale of the 62-item Mood and Anxiety Symptom Questionnaire, *MDD* major depressive disorder.

corrected repeated k-fold CV test) and had a 15.17% lower MSE relative to the null model.

GPM symptom prediction at 6-month follow-up

At 6-month follow-up, the GPM predicted (hypo)mania from the local efficiency of the left NAc during the RL task (Fig. 4A) [$N = 51$; GPM: $r = 0.487$, $p = 0.002$ permutation testing, MSE = 0.708; null model: $r = 0.400$, $p = 0.003$ permutation testing, MSE = 0.785]. Increased NAc efficiency was associated with greater (hypo)mania. The GPM outperformed the null model ($t = 6.36$, $p < 10^{-4}$ corrected repeated k-fold CV test) and had a 9.82% lower MSE relative to the null model. The GPM predicted anhedonia at 6-month follow-up from the centrality of the left caudate during resting-state (Fig. 4B) [$N = 64$; GPM: $r = 0.523$, $p = 2.1{\cdot}10^{-4}$ permutation testing, MSE = 164.23; null model: $r = 0.418$, $p = 7.4{\cdot}10^{-4}$ permutation testing, MSE = 187.16]. Increased centrality of the caudate was associated with greater anhedonia. The GPM outperformed the null model ($t = 4.75$, $p < 10^{-4}$ corrected repeated k-fold CV test) and had a 12.25% lower MSE relative to the null model.

GPM prediction using elastic-net

The inclusion of several graph-theoretical predictors by utilizing elastic-net did not result in an overall better predictive performance than the "winner-take-all" approach (Supplementary Results).

GPM using data-splitting: training on unipolar disorders and predicting for bipolar disorders

The GPM predicted anhedonia at baseline from the global efficiency of the functional connectome during the RL task [train (unipolar): $N = 45$; test (bipolar): $N = 16$; GPM: MSE = 172.59; null model: MSE = 247.90]. The GPM had a 30.38% lower MSE relative to the null model. The GPM predicted impulsivity at baseline from the centrality of the right ACC during resting-state [train (unipolar): $N = 53$; test (bipolar): $N = 20$; GPM: MSE = 177.53; null model: MSE = 202.27]. The GPM had a 12.23% lower MSE relative to the null model. Notably, these results are similar to the ones obtained on the whole transdiagnostic sample using cross-validation.

GPM external validation

For anhedonia at baseline, the GPM model defined on the primary sample's RL task data (using the global efficiency) predicted anhedonia scores for the validation sample during the MID task (Supplementary Fig. 1A) [$N = 37$; $r = 0.435$ $p = 0.007$]. For impulsivity at baseline, GPM model defined on the primary sample's resting-state (using the centrality of the left ACC) predicted impulsivity scores for the validation sample during resting-state (Supplementary Fig. 1B) [$N = 51$; $r = 0.348$ $p = 0.012$].

CPM symptom prediction

Baseline anhedonia was predicted from the CPM's negative-feature set during the RL task [$N = 61$; CPM: $r = 0.281$, $p = 0.020$ permutation testing, MSE = 164.34; null model: $r = 0.070$, $p = 0.161$ permutation testing, MSE = 172.15]. The CPM outperformed the null model ($t = 3.66$, $p = 1.3{\cdot}10^{-4}$ corrected repeated k-fold CV test) with a 4.54% lower MSE relative to the null model. Compared to the GPM, the CPM had a 7.69% higher MSE suggesting decreased performance, however, the difference between the models was not significant ($t = 1.19$, $p = 0.116$ corrected repeated k-fold CV test). Similar results were obtained with the positive-only weighted connectome (Supplementary Results). The CPM did not predict any other symptoms at baseline or follow-up.

DISCUSSION

Here, we developed and optimized a new brain-based model – the GPM – to predict symptoms in treatment-seeking individuals with mood disorders. Within the GPM, prediction was based on graph-theoretical measures of brain functional organization. We found that the efficiency and centrality of the reward circuit, specifically the ACC, caudate, and NAc, predicted symptoms of anhedonia, impulsivity, and (hypo)mania, cross-sectionally and prospectively. Importantly, cross-sectional predictive models

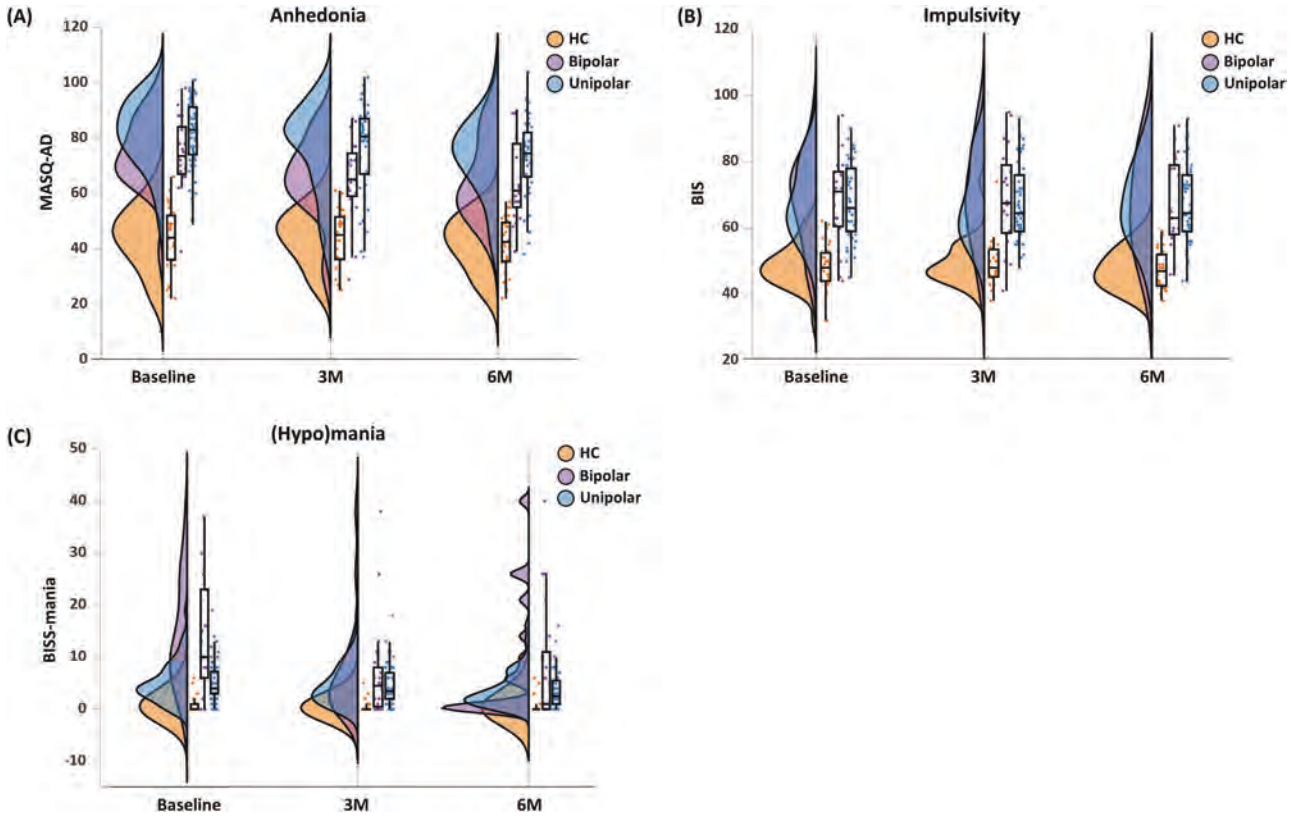

Fig. 2 Trajectories of anhedonia, impulsivity, and (hypo)mania symptoms. The distributions (using violin plots), scatter plots, and boxplots of **A** anhedonia, **B** impulsivity, and **C** (hypo)mania symptoms are presented for baseline, 3-month (3M) and 6-month (6M) follow-ups. A demographically matched group of 32 healthy controls (HC) (age = 28.40 ± 7.72, 17 female) is included for comparison.

generalized to an external validation sample, across different reward tasks, imaging protocols, and clinical characteristics.

Anhedonia at baseline was predicted by the GPM from the global efficiency of the functional connectome during the RL task. Greater anhedonia was associated with decreased global efficiency across the brain. Notably, a data-splitting analysis indicated that the prediction was cross-diagnostic: anhedonia in individuals with bipolar disorders was predicted after training the GPM on individuals with unipolar disorders. Anhedonia is one of the two cardinal symptoms of depression and is defined as a loss of pleasure, motivational drive, or lack of reactivity to pleasurable stimuli [48]. Global efficiency is a core network measure of integration and reflects the network's ability to pass information through short paths, which are considered important for the flow of signals and communication [49]. To the best of our knowledge, this is the first demonstrated link between anhedonia and global efficiency or integration. In agreement with our results, decreased global integration was reported in MDD [50].

Anhedonia at 6-month follow-up was predicted by the GPM from the centrality of the left caudate during resting-state. Greater anhedonia was associated with increased centrality of the caudate. Measures of centrality characterize the contribution of a brain region to the cohesiveness of the network [51]. There is emerging evidence associating anhedonia with increased centrality of the caudate. Specifically, a recent study found that centrality of the ventral striatum was positively associated with anhedonia at baseline, 2- and 4-year follow-ups [52].

Conversely, impulsivity was predicted at baseline by the GPM from the centrality of the left ACC during resting-state. Greater impulsivity was associated with increased ACC centrality. Critically, evidence of transdiagnostic generalization emerged: the GPM derived from individuals with unipolar disorders (centrality of the right ACC during resting-state) predicted baseline impulsivity among individuals with bipolar disorders. Impulsivity is a feature of several psychiatric disorders and can be defined as the tendency to act without adequate forethought or conscious judgment [53]. Several models have suggested that impulsivity is a heterogeneous construct composed of different dimensions. For example, the BIS divides impulsivity into three components: motor (acting without thinking), attentional (lack of focus on the task), and non-planning (orienting toward the present instead of the future).

The ACC has been suggested to play a key role in impulsivity, due to its involvement in diverse higher-order cognitive processes related to executive functioning [54]. In patients suffering from focal brain injuries, greater impulsivity was associated with lesions to the ACC [55]. Difficulties in perseverance, a subtype of impulsivity, were correlated with greater functional connectivity of the ACC with prefrontal regions [56]. In accordance with our findings, neuroimaging studies have supported the involvement of the ACC in the non-planning impulsivity subtype [57, 58].

(Hypo)mania at 6-month follow-up was predicted by the GPM from the local efficiency of the left NAc during the RL task, with greater (hypo)mania associated with increased NAc efficiency. Mania can be described as a distinct period of abnormally and persistently elevated, expansive, or irritable mood [30]. Notably, the NAc has been strongly implicated in manic symptoms. For example, transient (hypo)mania is the most commonly observed side effect after deep brain stimulation to the NAc [59–61]. Recently, preliminary evidence associated mania with increased structural connectivity [62] and functional connectivity [63] of the NAc.

For clinical translation, it is important to identify the cognitive state that maximizes the predictive accuracy of the GPM. Contrary to our hypothesis, the RL task did not amplify prediction, but rather a similar number of predictions was made from the RL task

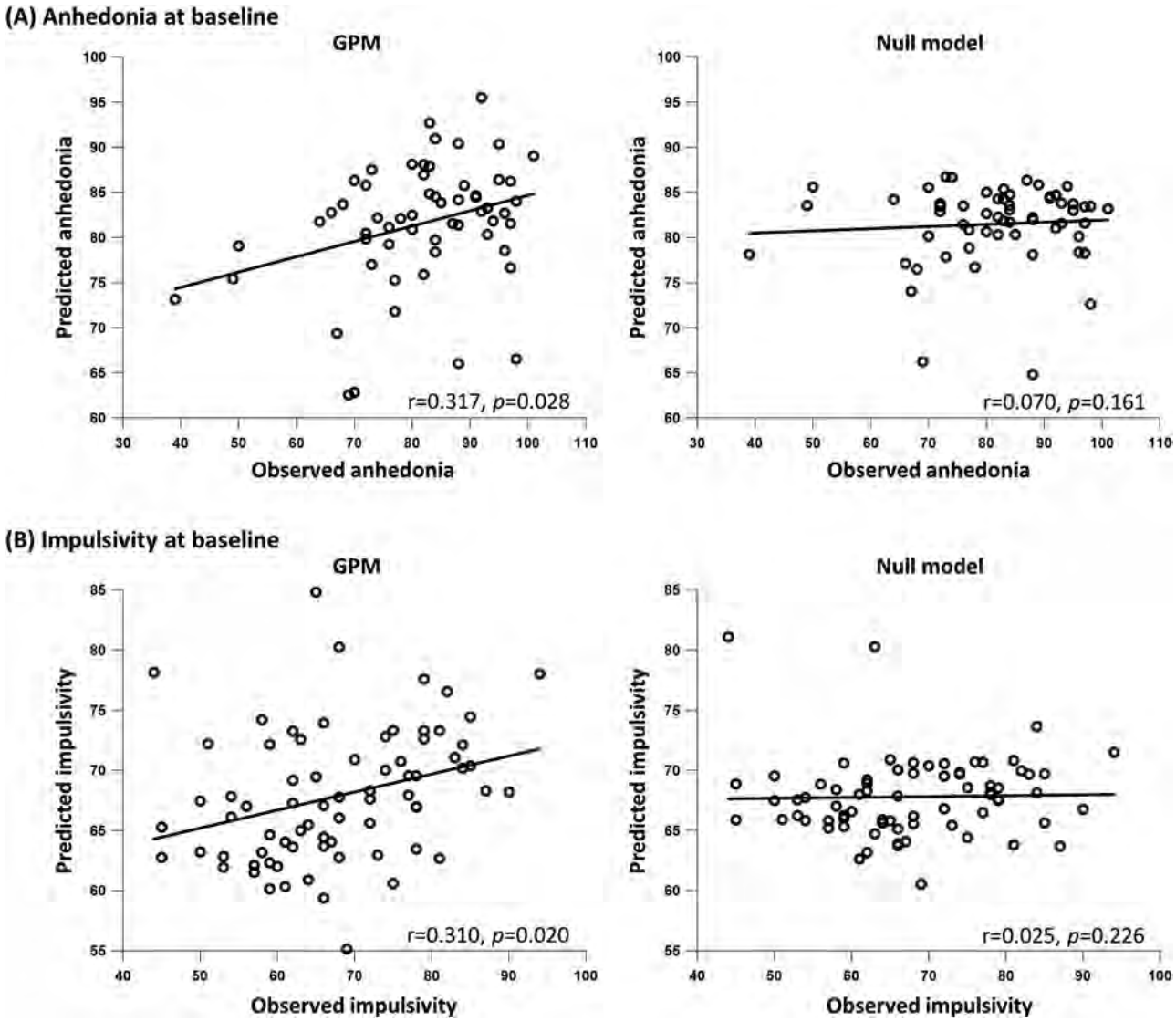

Fig. 3 The GPM predicted anhedonia and impulsivity at baseline. Predicted clinical scores (y axis) are presented as a function of the observed clinical scores (x axis). For each symptom, the predictions of the GPM are presented on the left panel and the predictions of the corresponding null model (without the brain predictor) are presented on the right panel. **A** Anhedonia was predicted by the GPM from the global efficiency of the functional connectome during the reinforcement-learning task. **B** Impulsivity was predicted by the GPM from the centrality of the left anterior cingulate cortex during resting-state. All *p* values were computed using permutation testing. Prediction was done while controlling for other baseline symptoms and medication load.

and resting-state. However, we note that the data for the two states were collected using different imaging sequences: single-band for the RL vs. multiband for the resting-state, and differed in scan duration and number of volumes. Thus, future investigations are needed to delineate more clearly the contribution of cognitive activities to the predictive accuracy of reward-related symptoms.

Most symptom predictions were based on regional network measures of the reward circuit, and not global ones, in accordance with our hypothesis. This finding resonates with numerous evidence for the pivotal role of the reward circuit in the pathophysiology of mood disorders [64] and extends previous literature by demonstrating the predictive utility of its network attributes. Importantly, different network measures were found to predict baseline symptoms and future ones. Since the ultimate goal of predictive modeling in psychiatry is to map future symptoms (and not baseline ones, which are generally known and can be assessed directly), our finding underscores the critical importance of longitudinal studies which monitor symptom trajectories. In addition, we note that the GPM outperformed the CPM for symptom prediction. This result was found when applying the CPM to either the functional connectome including negative weights, or the positive-only functional connectome.

Brain-based predictive modeling holds the cardinal promise to transcend the current paradigm of psychiatric assessments which are based solely on a patient's subjective report. An accurate, reproducible, predictive model can support important clinical decision making, such as selecting among possible treatments, initiating preventive strategies, and risk monitoring. While our study took a step toward achieving that goal, clearly more large-scale neuroimaging studies in individuals with mood disorders, with greater sample sizes, are essential to establish the predictive utility of the GPM. Nevertheless, our findings highlight several brain metrics that can be further tested as potential biomarkers, particularly for identifying individuals with depression that are at risk for developing bipolar symptoms. Although taking the leap

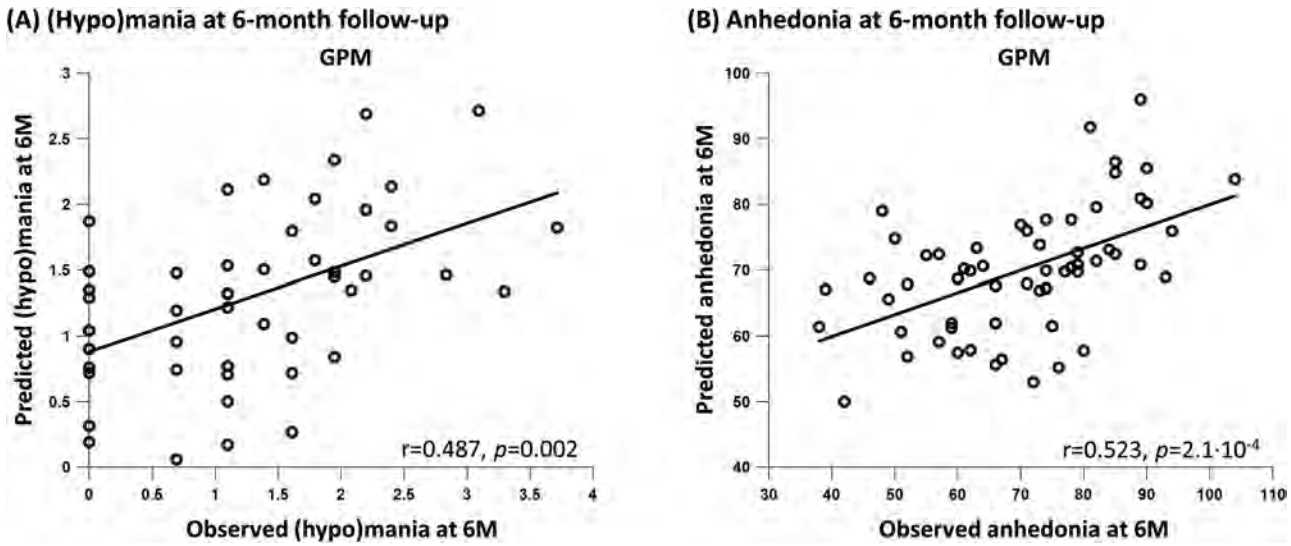

Fig. 4 The GPM predicted (hypo)mania and anhedonia at 6-month follow-up. Predicted clinical scores (y axis) are presented as a function of the observed clinical scores (x axis). **A** (Hypo)mania at 6-month (6M) follow-up was predicted by the GPM from the local efficiency of the left nucleus accumbens during the reinforcement-learning task. **B** Anhedonia at 6-month follow-up was predicted by the GPM from the centrality of the left caudate during resting-state. All *p* values were computed using permutation testing. Prediction was done while controlling for all baseline symptoms and medication load.

toward translational neuroscience is still rarely done, a few studies have directly investigated the clinical utility of neuroimaging biomarkers. For example, Kelley et al. assigned treatment for patients with MDD based on fluorodeoxyglucose positron emission tomography activity in the insula [65].

Several limitations should be noted. First, our samples were moderate in size and thus the findings should be carefully validated with larger datasets (though we obtained validation in an independent, external dataset). Second, the range of manic symptoms was relatively narrow and included mainly hypomania symptoms. Third, symptoms at 3-month follow-up were not predicted from brain measures due to high similarity with baseline scores (i.e., variance at 3 months was captured mostly by baseline scores). Moreover, impulsivity was quite stable across the 3 time-points. This may be due to the BIS capturing predominantly trait impulsivity. We note that a follow-up period of 6 months was chosen to facilitate the retention of participants, however, symptoms might change more substantially with longer follow-ups. Fourth, we did not test the influence of preprocessing choices or the parcellation atlas on predictive performance. Finally, alternative approaches to estimating functional connectomes may yield complementary information, e.g., aggregating fMRI data across paradigms (task and rest) [66], but were outside the scope of this investigation and merit future study. The optimal neuroimaging setting for detecting individual differences that are clinically relevant remains an ongoing research topic and an important direction for future research in psychiatry.

CONCLUSIONS

The GPM is an innovative tool that can map between clinical symptoms and network neuroimaging markers at the individual level. Across mood disorders, the GPM successfully predicted symptoms of anhedonic depression, impulsivity, and (hypo)mania, cross-sectionally and prospectively, from network features of the reward circuit. Ultimately, these results may have implications for prognostic indicators of mood symptoms. The clinical need is acute since a timely and effective treatment for individuals suffering from mood disorders, especially bipolar mood pathology, is crucial to reduce morbidity and mortality [67].

DATA AVAILABILITY

Datasets will be shared on reasonable request to the corresponding author.

CODE AVAILABILITY

The Brain Connectivity Toolbox was used for graph theoretical analyses and is freely available at https://sites.google.com/site/bctnet. The following functions were used: weight_conversion.m, clustering_coef_wu.m, efficiency_wei.m, distance_wei.m, charpath.m, betweenness_wei.m. Connectome-based predictive modeling (CPM) was done using MATLAB scripts available by Shen and colleagues [47].

REFERENCES

1. Hirschfeld RMA, Lewis L, Vornik LA. Perceptions and impact of bipolar disorder: How far have we really come? Results of the National Depressive and Manic-Depressive Association 2000 Survey of individuals with bipolar disorder. J Clin Psychiatry. 2003;64:161–74.
2. Ghaemi SN, Boiman EE, Goodwin FK. Diagnosing bipolar disorder and the effect of antidepressants: A naturalistic study. J Clin Psychiatry. 2000;61:804–8.
3. Angst J, Cui L, Swendsen J, Rothen S, Cravchik A, Kessler RC, et al. Major depressive disorder with subthreshold bipolarity in the national comorbidity survey replication. Am J Psychiatry. 2010;167:1194–201.
4. Sharma V, Khan M, Smith A. A closer look at treatment resistant depression: Is it due to a bipolar diathesis? J Affect Disord. 2005;84:251–7.
5. De Almeida JRC, Phillips ML. Distinguishing between unipolar depression and bipolar depression: Current and future clinical and neuroimaging perspectives. Biol Psychiatry. 2013;73:111–8.
6. Scheinost D, Noble S, Horien C, Greene AS, Lake EM, Salehi M, et al. Ten simple rules for predictive modeling of individual differences in neuroimaging. Neuroimage. 2019;193:35–45.
7. Siddiqi SH, Taylor SF, Cooke D, Pascual-Leone A, George MS, Fox MD. Distinct symptom-specific treatment targets for circuit-based neuromodulation. Am J Psychiatry. 2020;177:435–46.
8. Scheinost D, Hsu TW, Avery EW, Hampson M, Constable RT, Chun MM, et al. Connectome-based neurofeedback: A pilot study to improve sustained attention. Neuroimage. 2020;212:116684.
9. Finn ES, Shen X, Scheinost D, Rosenberg MD, Huang J, Chun MM, et al. Functional connectome fingerprinting: Identifying individuals using patterns of brain connectivity. Nat Neurosci. 2015;18:1664–71.
10. Beaty RE, Kenett YN, Christensen AP, Rosenberg MD, Benedek M, Chen Q, et al. Robust prediction of individual creative ability from brain functional connectivity. Proc Natl Acad Sci USA. 2018;115:1087–92.
11. Chen J, Tam A, Kebets V, Orban C, Ooi LQR, Asplund CL, et al. Shared and unique brain network features predict cognitive, personality, and mental health scores in the ABCD study. Nat Commun. 2022;13:1–17.

12. Greene AS, Gao S, Scheinost D, Constable RT. Task-induced brain state manipulation improves prediction of individual traits. Nat Commun. 2018;9:1–13.
13. Horien C, Floris DL, Greene AS, Noble S, Rolison M, Tejavibulya L, et al. Functional connectome–based predictive modeling in autism. Biol Psychiatry. 2022;92:626–42.
14. Ibrahim K, Noble S, He G, Lacadie C, Crowley MJ, McCarthy G, et al. Large-scale functional brain networks of maladaptive childhood aggression identified by connectome-based predictive modeling. Mol Psychiatry. 2022;27:985–99.
15. Yip SW, Scheinost D, Potenza MN, Carroll KM. Connectome-based prediction of cocaine abstinence. Am J Psychiatry. 2019;176:156–64.
16. Medaglia JD, Lynall ME, Bassett DS. Cognitive network neuroscience. J Cogn Neurosci. 2015;27:1471–91.
17. Dong D, Li C, Ming Q, Zhong X, Zhang X, Sun X, et al. Topologically state-independent and dependent functional connectivity patterns in current and remitted depression. J Affect Disord. 2019;250:178–85.
18. He H, Yu Q, Du Y, Vergara V, Victor TA, Drevets WC, et al. Resting-state functional network connectivity in prefrontal regions differs between unmedicated patients with bipolar and major depressive disorders. J Affect Disord. 2016;190:483–93.
19. Jacob Y, Morris LS, Huang KH, Schneider M, Rutter S, Verma G, et al. Neural correlates of rumination in major depressive disorder: A brain network analysis. NeuroImage Clin. 2020;25:102142.
20. Kim K, Kim SW, Myung W, Han CE, Fava M, Mischoulon D, et al. Reduced orbitofrontal-thalamic functional connectivity related to suicidal ideation in patients with major depressive disorder. Sci Rep. 2017;7:15772.
21. Sheng J, Shen Y, Qin Y, Zhang L, Jiang B, Li Y, et al. Spatiotemporal, metabolic, and therapeutic characterization of altered functional connectivity in major depressive disorder. Hum Brain Mapp. 2018;39:1957–71.
22. Gong L, Hou Z, Wang Z, He C, Yin Y, Yuan Y, et al. Disrupted topology of hippocampal connectivity is associated with short-term antidepressant response in major depressive disorder. J Affect Disord. 2018;225:539–44.
23. Spielberg JM, Sadeh N, Cha J, Matyi MA, Anand A. Affect regulation–related emergent brain network properties differentiate depressed bipolar disorder from major depression and track risk for bipolar disorder. Biol Psychiatry Cogn Neurosci Neuroimaging. 2022;7:765–73.
24. Manelis A, Almeida JRC, Stiffler R, Lockovich JC, Aslam HA, Phillips ML. Anticipation-related brain connectivity in bipolar and unipolar depression: A graph theory approach. Brain. 2016;139:2554–66.
25. Rubinov M, Sporns O. Complex network measures of brain connectivity: Uses and interpretations. Neuroimage. 2010;52:1059–69.
26. Insel T, Cuthbert B, Garvey M, Heinssen R, Pine DS, Quinn K, et al. Research Domain Criteria (RDoC): Toward a new classification framework for research on mental disorders. Am J Psychiatry. 2010;167:748–51.
27. Greene AS, Gao S, Scheinost D, Constable RT. Task-induced brain state manipulation improves prediction of individual traits. Nat Commun. 2018;9:2807.
28. Pizzagalli DA, Jahn AL, O'Shea JP. Toward an objective characterization of an anhedonic phenotype: A signal-detection approach. Biol Psychiatry. 2005;57:319–27.
29. Whitton AE, Kumar P, Treadway MT, Rutherford AV, Ironside ML, Foti D, et al. Mapping disease course across the mood disorder spectrum through a research domain criteria framework. Biol Psychiatry Cogn Neurosci Neuroimaging. 2021;6:706–15.
30. First M, Spitzer R, Gibbon M, Williams J Structured Clinical Interview for DSM IV-TR Axis I Disorders, Research Version, Patient Edition (SCID-I/P). New York: New York State Psychiatric Institute; (2002).
31. Pessiglione M, Seymour B, Flandin G, Dolan RJ, Frith CD. Dopamine-dependent prediction errors underpin reward-seeking behaviour in humans. Nature. 2006;442:1042–5.
32. Whitton AE, Kumar P, Treadway MT, Rutherford A, Ironside ML, Foti D, et al. Distinct profiles of anhedonia and reward processing and their prospective associations with quality of life among individuals with mood disorders. Mol Psychiatry. https://doi.org/10.1038/s41380-023-02165-1 (2023).
33. Watson D, Weber K, Assenheimer JS, Clark LA, Strauss ME, McCormick RA. Testing a tripartite model: I. Evaluating the convergent and discriminant validity of anxiety and depression symptom scales. J Abnorm Psychol. 1995;104:3–14.
34. Patton JH, Stanford MS, Barratt ES. Factor structure of the barratt impulsiveness scale. J Clin Psychol. 1995;51:768–74.
35. Gonzalez JM, Bowden CL, Katz MM, Thompson P, Singh V, Prihoda TJ, et al. Development of the bipolar inventory of symptoms scale: Concurrent validity, discriminant validity and retest reliability. Int J Methods Psychiatr Res. 2008;17:198–209.
36. Esteban O, Markiewicz CJ, Blair RW, Moodie CA, Isik AI, Erramuzpe A, et al. fMRIPrep: a robust preprocessing pipeline for functional MRI. Nat Methods. 2019;16:111–6.
37. Whitfield-Gabrieli S, Nieto-Castanon A. Conn: a functional connectivity toolbox for correlated and anticorrelated brain networks. Brain Connect. 2012;2:125–41.
38. Schaefer A, Kong R, Gordon EM, Laumann TO, Zuo XN, Holmes AJ, et al. Local-global parcellation of the human cerebral cortex from intrinsic functional connectivity mri. Cereb Cortex. 2018;28:3095–114.
39. Desikan RS, Ségonne F, Fischl B, Quinn BT, Dickerson BC, Blacker D, et al. An automated labeling system for subdividing the human cerebral cortex on MRI scans into gyral based regions of interest. Neuroimage. 2006;31:968–80.
40. Sackeim HA. The definition and meaning of treatment-resistant depression. J Clin Psychiatry. 2001;62:10–17.
41. Bouckaert RR, Frank E. Evaluating the replicability of significance tests for comparing learning algorithms. Pacific-Asia conference on knowledge discovery and data mining. Berlin, Heidelberg: Springer Berlin Heidelberg. (2004).
42. Zou H, Hastie T. Regularization and variable selection via the elastic net. J R Stat Soc Ser B Stat Methodol. 2005;67:301–20.
43. Qian J, Hastie T, Friedman J, Tibshirani R, Simon N. Glmnet for Matlab. http://hastie.su.domains/glmnet_matlab/ (2013).
44. Belleau EL, Bolton TAW, Kaiser RH, Clegg R, Cárdenas E, Goer F, et al. Resting state brain dynamics: Associations with childhood sexual abuse and major depressive disorder. NeuroImage Clin. 2022;36:103164.
45. Liu Y, Admon R, Mellem MS, Belleau EL, Kaiser RH, Clegg R, et al. Machine learning identifies large-scale reward-related activity modulated by dopaminergic enhancement in major depression. Biol Psychiatry Cogn Neurosci Neuroimaging. 2020;5:163–72.
46. Knutson B, Westdorp A, Kaiser E, Hommer D. FMRI visualization of brain activity during a monetary incentive delay task. Neuroimage. 2000;12:20–27.
47. Shen X, Finn ES, Scheinost D, Rosenberg MD, Chun MM, Papademetris X, et al. Using connectome-based predictive modeling to predict individual behavior from brain connectivity. Nat Protoc. 2017;12:506–18.
48. Pizzagalli DA. Toward a better understanding of the mechanisms and pathophysiology of Anhedonia: Are we ready for translation? Am J Psychiatry. 2022;179:458–69.
49. Sporns O. Graph theory methods: Applications in brain networks. Dialogues Clin Neurosci. 2018;20:111–20.
50. Yang H, Chen X, Chen ZB, Li L, Li XY, Castellanos FX, et al. Disrupted intrinsic functional brain topology in patients with major depressive disorder. Mol Psychiatry. 2021;26:7363–71.
51. Borgatti SP, Everett MG. A Graph-theoretic perspective on centrality. Soc Networks. 2006;28:466–84.
52. Pan PM, Sato JR, Paillère Martinot ML, Martinot JL, Artiges E, Penttilä J, et al. Longitudinal trajectory of the link between Ventral Striatum and depression in adolescence. Am J Psychiatry. 2022;179:470–81.
53. Moeller FG, Barratt ES, Dougherty DM, Schmitz JM, Swann AC. Psychiatric aspects of impulsivity. Am J Psychiatry. 2001;158:1783–93.
54. Castellanos-Ryan N, Séguin JR. Prefrontal and anterior cingulate cortex mechanisms of impulsivity. Oxford Handbook. Externalizing Spectr. Disord., Oxford University Press; (2015).
55. McDonald V, Hauner KK, Chau A, Krueger F, Grafman J. Networks underlying trait impulsivity: Evidence from voxel-based lesion-symptom mapping. Hum Brain Mapp. 2017;38:656–65.
56. Golchert J, Smallwood J, Jefferies E, Liem F, Huntenburg JM, Falkiewicz M, et al. In need of constraint: Understanding the role of the cingulate cortex in the impulsive mind. Neuroimage. 2017;146:804–13.
57. Kaasinen V, Honkanen EA, Lindholm K, Jaakkola E, Majuri J, Parkkola R, et al. Serotonergic and dopaminergic control of impulsivity in gambling disorder. Addict Biol. 2023;28:28.
58. Cohen-Gilbert JE, Sneider JT, Crowley DJ, Rosso IM, Jensen JE, Silveri MM. Impact of family history of alcoholism on glutamine/glutamate ratio in anterior cingulate cortex in substance-naïve adolescents. Dev Cogn Neurosci. 2015;16:147–54.
59. Okun MS, Mann G, Foote KD, Shapira NA, Bowers D, Springer U, et al. Deep brain stimulation in the internal capsule and nucleus accumbens region: Responses observed during active and sham programming. J Neurol Neurosurg Psychiatry. 2007;78:310–4.
60. De Koning PP, Figee M, Van Den Munckhof P, Schuurman PR, Denys D. Current status of deep brain stimulation for obsessive-compulsive disorder: A clinical review of different targets. Curr Psychiatry Rep. 2011;13:274–82.
61. Kim Y, McGee S, Czeczor JK, Walker AJ, Kale RP, Kouzani AZ, et al. Nucleus accumbens deep-brain stimulation efficacy in ACTH-pretreated rats: Alterations in mitochondrial function relate to antidepressant-like effects. Transl Psychiatry. 2016;6:e842.
62. Damme KS, Young CB, Nusslock R. Elevated nucleus accumbens structural connectivity associated with proneness to hypomania: A reward hypersensitivity perspective. Soc Cogn Affect Neurosci. 2017;12:928–36.
63. Whittaker JR, Foley SF, Ackling E, Murphy K, Caseras X. The functional connectivity between the nucleus accumbens and the ventromedial prefrontal cortex as an endophenotype for bipolar disorder. Biol Psychiatry. 2018;84:803–9.

64. Russo SJ, Nestler EJ. The brain reward circuitry in mood disorders. Nat Rev Neurosci. 2013;14:609–25.
65. Kelley ME, Choi KS, Rajendra JK, Craighead WE, Rakofsky JJ, Dunlop BW, et al. Establishing evidence for clinical utility of a neuroimaging biomarker in major depressive disorder: prospective testing and implementation challenges. Biol Psychiatry. 2021;90:236–42.
66. Elliott ML, Knodt AR, Cooke M, Kim MJ, Melzer TR, Keenan R, et al. General functional connectivity: Shared features of resting-state and task fMRI drive reliable and heritable individual differences in functional brain networks. Neuroimage. 2019;189:516–32.
67. McIntyre RS, Berk M, Brietzke E, Goldstein BI, López-Jaramillo C, Kessing LV, et al. Bipolar disorders. Lancet. 2020;396:1841–56.

AUTHOR CONTRIBUTIONS

RD: Conceptualization; Data curation; Formal analysis; Investigation; Methodology; Resources; Software; Visualization; Writing - Original draft; Writing – Review & Editing. AEW: Conceptualization; Investigation; Project administration; Methodology; Resources; Writing – Review & Editing. MTT: Investigation; Project administration; Resources; Writing – Review & Editing. AVR: Investigation; Project administration; Resources; Writing – Review & Editing. PK: Investigation; Project administration; Resources; Writing – Review & Editing. MLI: Investigation; Project administration; Resources; Writing – Review & Editing. RHK: Investigation; Project administration; Resources; Writing – Review & Editing. BR: Methodology; Writing – Review & Editing. DAP: Conceptualization; Funding acquisition; Methodology; Resources; Supervision; Writing – Review & Editing.

FUNDING

The study was supported by the National Institute of Mental Health (NIMH) (Grant Nos. R01 MH101521 and R37 MH068376 to DAP). RD is an Awardee of the Weizmann Institute of Science – Israel National Postdoctoral Award Program for Advancing Women in Science. AEW was supported by a National Health and Medical Research Council Investigator Grant (GNT 2017521). Biostatistical consultation was provided by Harvard Catalyst.

COMPETING INTERESTS

Over the past 3 years, Dr. Pizzagalli has received consulting fees from Boehringer Ingelheim, Compass Pathways, Engrail Therapeutics, Neumora Therapeutics (formerly BlackThorn Therapeutics), Neurocrine Biosciences, Neuroscience Software, Otsuka, Sage Therapeutics, Sama Therapeutics, Sunovion, and Takeda; he has received honoraria from the American Psychological Association, Psychonomic Society and Springer (for editorial work) and from Alkermes; he has received research funding from the Bird Foundation, Brain and Behavior Research Foundation, Dana Foundation, Wellcome Leap, Millennium Pharmaceuticals, and NIMH; he has received stock options from Compass Pathways, Engrail Therapeutics, Neumora Therapeutics, and Neuroscience Software; he has a financial interest in Neumora Therapeutics, which has licensed the copyright to the human version of the probabilistic reward task through Harvard University. No funding from these entities was used to support the current work, and all views expressed are solely those of the authors. All other authors have no conflicts of interest or relevant disclosures.

ADDITIONAL INFORMATION

Supplementary information The online version contains supplementary material available at https://doi.org/10.1038/s41386-024-01842-1.

Correspondence and requests for materials should be addressed to Diego A. Pizzagalli.

Brain-based graph-theoretical predictive modeling to map the trajectory of anhedonia, impulsivity, and hypomania from the human functional connectome

Supplemental Information

Supplemental Methods

- Inclusion/exclusion criteria
- MRI data acquisition
- MRI data preprocessing
- fMRI data denoising
- Graph theory measures
- Assessment of predictive performance
- GPM utilizing elastic-net algorithm
- GPM external validation analysis
- Illustration of the differences between the brain-based graph-theoretical predictive model (GPM) and connectome-based predictive modeling (CPM)

Supplemental Results

- Supplemental Table 1. List of medications used by participants
- Supplemental Table 2. Correlations among symptoms over time
- GPM prediction using 10-fold cross-validation
- GPM prediction using elastic-net ("GPM elastic-net")
- Supplemental Figure 1. GPM external validation
- CPM prediction from the positive-only functional connectome

Supplemental Methods

Inclusion/exclusion criteria

Non-psychotic individuals seeking treatment for mood pathology were recruited from the Depression Clinical and Research Center and the Bipolar Clinical and Research Center at Massachusetts General Hospital, as well as the Center for Depression, Anxiety and Stress Research at McLean Hospital. Clinical diagnoses and eligibility were evaluated using the Structured Clinical Interview for DSM-IV conducted by master's or Ph.D.-level clinical interviewers.

Inclusion criteria:

1. Ability to provide written, informed consent
2. Normal or corrected-to-normal vision and hearing
3. Fluency in written and spoken English
4. Depressive or hypomanic symptoms severe enough to cause distress or impairment, and warrant intervention
5. The depressive or hypomanic symptoms are not secondary to another Axis-I DSM-IV psychiatric disorder, or due to the effects of a substance
6. Absence of psychotropic medication for at least two weeks or stable antidepressant or mood stabilizing medication over the past 8 weeks

Exclusion criteria:

1. Left-handed or ambidextrous
2. Current drug use (cocaine, cannabis, opiates, amphetamines, benzodiazepines, barbiturates), as indicated by a positive urine drug screen on the day of testing
3. Current use of medications with potent dopaminergic effects, including stimulants or antipsychotics, or any use of antidopaminergic medications in the past 6 months
4. Recent use of any medication that affects blood flow or pressure
5. Current use of antibiotics
6. Pregnancy (as indicated by urine pregnancy test on the day of the MRI scan)

7. Serious unstable medical illness
8. Self-reported hypothyroidism
9. History or current diagnosis of dementia
10. A score of < 25 on the Mini Mental State Exam
11. History of chronic migraine (>15 days/month) or seizure disorder
12. History of significant head injury or loss of consciousness for 2 minutes or longer
13. MRI contraindications
14. A current diagnosis of obsessive-compulsive disorder (OCD), bulimia, alcohol dependence, substance abuse, or substance dependence
15. A history or current diagnosis of a psychotic disorder, stimulant dependence, or anorexia
16. Suicidal ideation where outpatient treatment is determined unsafe by the study clinical interviewer
17. Electroconvulsive therapy within the past two years

MRI data acquisition

Reinforcement-learning (RL) task data were acquired using a single-band gradient-echo echo-planar imaging (GE-EPI) sequence with the following parameters: TR=3 sec, TE=30 ms, image matrix=64×64, in-plane field of view=224x224 mm, flip angle=75°, voxel size=3.5x3.5x2 mm, 57 interleaved slices with a GRAPPA factor of 2. The RL task included three runs, each consisting of 210 measurements. Resting-state data were acquired using a multiband GE-EPI sequence with the following parameters: TR=0.5 sec, TE=30 ms, image matrix=64×64, in-plane field of view=220x220 mm, flip angle=43°, voxel size=3.4x3.4x3 mm, 48 interleaved slices with a multiband factor of 16, and 800 measurements. All functional images were acquired with a 30-degree titled slice acquisition to mitigate signal loss in regions affected by susceptibility artifacts. Anatomical images were acquired using a high-resolution T1-weighted multi-echo MPRAGE sequence with TR=2.2 sec, TE= 1.54, 3.36, 5.18, 7ms, in-plane field of view=230x230 mm, voxel size=1.2x1.2x1.2 mm, 144 slices. The T1-weighted images were acquired for coregistration and normalization of the functional images.

MRI data preprocessing

Preprocessing of MRI data (anatomical, RL task, resting-state) was done in fMRIPrep 20.2.1 [1]. The following description of the preprocessing steps was taken from the custom language generated by fMRIPrep, which is recommended for use in publications and has been released under the CC0 license. *Anatomical data preprocessing:* The T1-weighted (T1w) image was corrected for intensity non-uniformity (INU) with N4BiasFieldCorrection (Tustison et al. 2010), distributed with ANTs 2.3.3 (Avants et al. 2008), and used as T1w-reference throughout the workflow. The T1w-reference was then skull-stripped with a Nipype implementation of the antsBrainExtraction.sh workflow (from ANTs), using OASIS30ANTs as target template. Brain tissue segmentation of cerebrospinal fluid (CSF), white-matter (WM) and gray-matter (GM) was performed on the brain-extracted T1w using fast (FSL 5.0.9, Zhang, Brady, and Smith 2001). Brain surfaces were reconstructed using recon-all (FreeSurfer 6.0.1, Dale, Fischl, and Sereno 1999), and the brain mask estimated previously was refined with a custom variation of the method to reconcile ANTs-derived and FreeSurfer-derived segmentations of the cortical gray-matter of Mindboggle (Klein et al. 2017). Volume-based spatial normalization to two standard spaces (MNI152NLin2009cAsym, MNI152NLin6Asym) was performed through nonlinear registration with antsRegistration (ANTs 2.3.3), using brain-extracted versions of both T1w reference and the T1w template. The following templates were selected for spatial normalization: ICBM 152 Nonlinear Asymmetrical template version 2009c [Fonov et al. (2009), TemplateFlow ID: MNI152NLin2009cAsym], FSL's MNI ICBM 152 non-linear 6th Generation Asymmetric Average Brain Stereotaxic Registration Model [Evans et al. (2012), TemplateFlow ID: MNI152NLin6Asym].

Functional data preprocessing: The following preprocessing was performed for all functional images. First, a reference volume and its skull-stripped version were generated by aligning and averaging 1 single-band references (SBRefs). A deformation field to correct for susceptibility distortions was estimated based on fMRIPrep's fieldmap-less approach. The deformation field is that resulting from co-registering the BOLD reference to the same-subject T1w-reference with its intensity inverted (Wang et al. 2017; Huntenburg 2014). Registration is performed with antsRegistration (ANTs 2.3.3), and the process

regularized by constraining deformation to be nonzero only along the phase-encoding direction and modulated with an average fieldmap template (Treiber et al. 2016). Based on the estimated susceptibility distortion, a corrected EPI (echo-planar imaging) reference was calculated for a more accurate co-registration with the anatomical reference. The BOLD reference was then co-registered to the T1w reference using bbregister (FreeSurfer) which implements boundary-based registration (Greve and Fischl 2009). Co-registration was configured with six degrees of freedom. Head-motion parameters with respect to the BOLD reference (transformation matrices, and six corresponding rotation and translation parameters) are estimated before any spatiotemporal filtering using mcflirt (FSL 5.0.9, Jenkinson et al. 2002). BOLD runs were slice-time corrected using 3dTshift from AFNI 20160207 (Cox and Hyde 1997). First, a reference volume and its skull-stripped version were generated using a custom methodology of fMRIPrep. The BOLD time-series were resampled onto the following surfaces (FreeSurfer reconstruction nomenclature): fsaverage. The BOLD time-series (including slice-timing correction when applied) were resampled onto their original, native space by applying a single, composite transform to correct for head-motion and susceptibility distortions. The BOLD time-series were resampled into standard space, generating a preprocessed BOLD run in MNI152NLin2009cAsym space.

fMRI data denoising

Further denoising of the fMRI data (RL task and rest) was done in CONN toolbox [2]. The anatomical component-based noise correction (aCompCor) [3] was used to regress out potential confounds. These included: (i) outlier scans, removed by censoring [4]. Outlier scans were identified based on the amount of subject in-scanner motion as measured by the framewise displacement (FD) and global BOLD signal. Acquisitions with FD > 0.9mm or global BOLD signal changes > 5 standard deviations were considered outliers and removed by regression. (ii) First 5 principal components (PCAs) of the CSF and white matter signals: were regressed out to minimize the effects of physiological non-neuronal signals such as cardiac and respiratory signals. (iii) Estimated subject-motion parameters and their first-order derivatives (a total of 12 parameters). (iv) Session effects: The potential effects of the beginning of the session were removed

by a step function convolved with the hemodynamic response function, in addition to the linear BOLD signal trend. Note that global signal regression was not performed. After regression of all potential confounding effects, temporal band-pass filtering (0.008-0.09 Hz) was performed.

One participant was excluded from both paradigms (RL task, rest) due to lack of fMRI data (lost to follow-up after baseline clinical session). For the RL task, 18 participants were excluded due to: in-scanner motion, i.e., >20% outlier volumes (n=15), missing data (n=2), and falling asleep during the task (n=1). All participants passed QA for the resting-state. The final analyzed sample included 79 participants (57 with unipolar disorders, 22 with bipolar disorders) for the resting-state and 61 participants (45 with unipolar disorders, 16 with bipolar disorders) for the RL task. Note that one individual with bipolar disorder was excluded in previous work [5,6] due to lack of RL task data, and another individual with bipolar disorder was included in previous analyses [5,6] but excluded here due to lack of fMRI data.

Graph theory measures

Graph theoretical measures can be grouped into measures of integration, segregation, and centrality [7]. (i) *Integration*: the ability to rapidly combine information across remote brain regions. It includes the characteristic path length which is the average shortest path length between all pairs of nodes and global efficiency which is the average inverse shortest path length. (ii) *Segregation:* quantifies the presence of densely interconnected brain regions and includes the clustering coefficient and local efficiency. The clustering coefficient is the fraction of a node's neighbors (nodes that are directly connected to the node) that are also neighbors of each other. The local efficiency is the efficiency of the subgraph of a node that contains only its neighbors. (iii) *Centrality:* the importance of a region for efficient communication. It includes betweenness centrality, which is the fraction of the shortest paths that pass through a node.

Assessment of predictive performance

Predictive performance (the correspondence between predicted and observed scores) was evaluated by the mean squared error (MSE). The MSE is defined as the average sum of the squared difference between the

observed and predicted values and measures the variance of the residuals, with a smaller MSE indicating a better model. To quantify the contribution of the graph-theoretical brain predictor beyond that of baseline symptoms, we compared the GPM to a corresponding cross-validated null model. The null model was defined as the same model without the graph-theoretical brain predictor, including only baseline symptoms and psychotropic medication load. To formally compare between the GPM and null models, the corrected repeated k-fold cv test was used [39]. In addition, the relative difference in the MSE between the models was derived as follows: MSE_diff=(MSE_null-MSE_GPM)/MSE_null. The same procedure was used to evaluate the predictive accuracy of the CPM. Last, since correlation is the most commonly reported metric of prediction performance in fMRI literature, we computed Pearson's correlation between predicted and observed scores. The statistical significance of correlation was assessed using permutation testing, i.e., the observed scores were randomly shuffled between participants, and the prediction process was repeated 10,000 times to generate a null distribution.

GPM utilizing elastic-net algorithm

As an alternative approach to the feature-selection step of the GPM, we tested the inclusion of several graph-theoretical metrics by utilizing an elastic-net algorithm to generate the predictive model. Elastic-net is a hybrid of ridge regression and lasso regularization and can be used to select the important predictors among a large set [8]. Elastic-net was implemented using *Glmnet* package for MATLAB (http://hastie.su.domains/glmnet_matlab/) [9]. Hyper-parameters were optimized using cross-validation for all possible combinations of alpha (elastic net penalty, ranging from 0 to 1 in steps of 0.05) and lambda (controls the overall strength of penalty). The model with the best alpha-lambda pair that minimized the cross-validated error was selected.

GPM external validation analysis

The generalizability of cross-sectional models was tested on an independent sample of 96 unmedicated individuals (ages: 18-48; 77 female), including 44 MDD and 52 HC. This sample combined two datasets that used the same imaging sequences [10,11]. Impulsivity scores were available for a subset of 53 individuals (25 MDD, 28 HC). (Hypo)mania symptoms were not assessed. Functional MRI data were collected for two conditions: (i) resting-state and (ii) a reward processing task: the Monetary Incentive Delay task (MID) [12]. Models were built on the primary sample and prediction was tested on the external sample. Note that since the clinical measures used to compute the null model (i.e., other baseline symptoms and medication load) were mostly not available for this sample, a null model was not computed, and thus prediction success was assessed using Pearsons's correlation and *p* values. The MSE is a relative number and is more informative when comparing between models (i.e., GPM and null models). Further details are provided below:

Assessment of symptoms

Symptoms were evaluated using the same clinical scales administered to the primary sample. Namely, anhedonia was assessed using the Anhedonic Depression subscale of the 62-item Mood and Anxiety Symptom Questionnaire (MASQ-AD) [13] and impulsivity was assessed using the Barratt Impulsiveness Scale (BIS) [14].

MRI data acquisition

MRI data were collected at the McLean Imaging Center on the same MRI scanner used for the primary sample, i.e., a 3T Siemens Tim Trio using a 32-channel head coil. MID task data were acquired using the same single-band GE-EPI sequence used for the RL task of the primary sample, with a total of 461 measurements. Resting-state data used a different sequence than that of the primary sample, i.e., a single-band GE-EPI sequence with the following parameters: TR=3 sec, TE=30 ms, image matrix=72×72, in-plane field of view=216x216 mm, flip angle=85°, voxel size=3x3x3 mm, 47 interleaved slices, with a total of 124 measurements. Anatomical images were acquired with the same multi-echo MPRAGE sequence used for the primary sample.

MRI data preprocessing

Preprocessing of MRI data followed the same pipeline used for the primary sample.

Dopamine/placebo manipulation

Before the onset of the MRI scan, the external sample underwent a pharmacological manipulation in a double-blind placebo-controlled design, where participants received either a single dose of 50 mg amisulpride (hypothesized to increase dopaminergic signaling via autoreceptor blockade) or a placebo pill. Validation analysis was conducted on the external sample across pharmacological conditions (dopamine, placebo).

Prediction of anhedonia

Due to the bimodal distribution of anhedonia scores across the MDD and HC samples, prediction of anhedonia was done only for individuals with MDD. Six individuals with MDD were excluded due to in-scanner motion (>20% outlier volumes) and 1 participant was further identified as an outlier in their graph metric scores and removed, yielding a final analyzed sample of 37 individuals with MDD. Impulsivity scores were not accounted for since they were available for only a subsample of 22 individuals with MDD. Note that for the external sample, data were collected during the MID instead of the RL task used for the primary sample [15]. Since both tasks probe reward processing, the model was built on the RL task and prediction was tested on the MID.

Prediction of impulsivity

Impulsivity scores were distributed normally across individuals with MDD and HC, thus, prediction was done using the whole sample. This choice was made to increase the sample size, since impulsivity scores were available for only a subset of the external sample (53 individuals; 25 MDD, 28 HC). Two individuals with MDD were excluded due to in-scanner motion (>20% outlier volumes), yielding a final analyzed sample of 51 individuals (23 MDD, 28 HC). Anhedonia scores were available for all individuals and accounted for in the predictive model.

Illustration of the differences between the GPM and CPM

Below are illustrations of the GPM and the CPM, to enable a visual comparison of their similarities and differences. Note that the models differ in steps 2 and 3 (highlighted by the red frame).

(i) The CPM

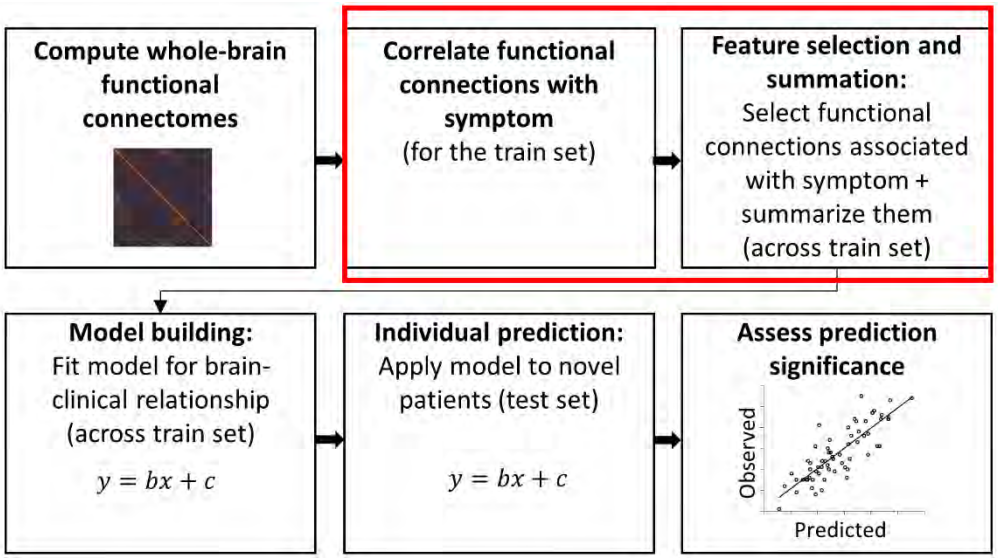

The Figure was modified after Shen et al. [16]

(ii) The GPM

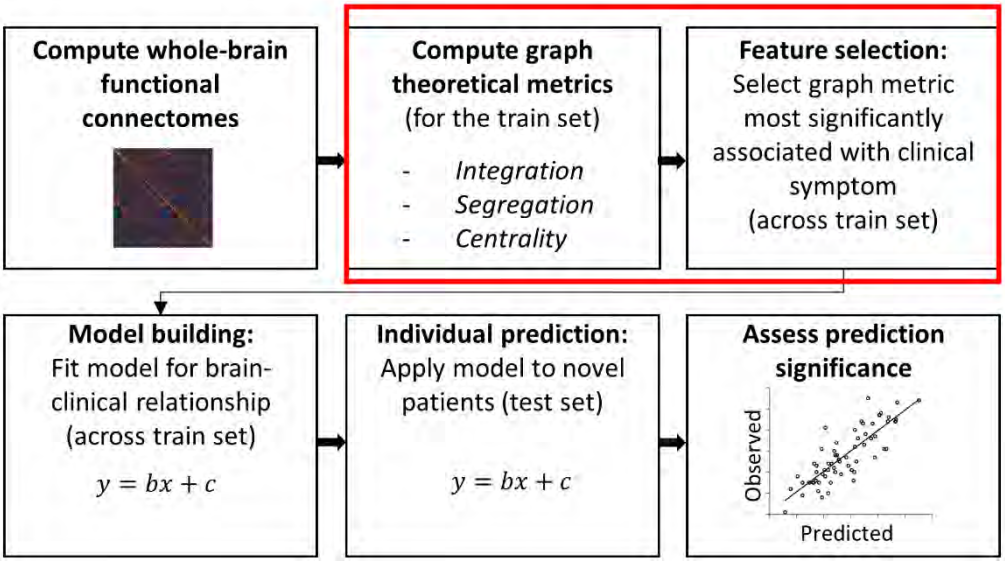

Supplemental Results

Supplemental Table 1. List of medications used by participants

Each row refers to a single participant. The rest of the sample was not taking medications.

Unipolar disorders
Lithium (300 mg/day)
Sertraline (50 mg/day); Wellbutrin (200 mg/day)
Celexa (5 mg/day)
Celexa (20 mg/day); Remeron (15 mg/day)
Zoloft (50 mg/day)
Klonopin (2 mg/day); Effexor (150 mg/day)
Prozac (20 mg/day)
Vilazodone (10 mg/day); Wellbutrin (300 mg/day)
Sertraline (200 mg/day)
Celexa (20 mg/day)
Cymbalta (60 mg/day); Wellbutrin (200 mg/day)
Fluvoxamine (300 mg/day); Trazadone (25 mg/day)
Sertraline (150 mg/day)
Lexapro (20 mg/day)
Sertraline (200 mg/day)
Wellbutrin (200 mg/day)
Prozac (20 mg/day)
Lexapro (10 mg/day)
Paxil (30 mg/day)
Zoloft (150 mg/day)
Bipolar disorders
Depakote (1250 mg/day); Bupropion (450 mg/day); Seroquel (400-500 mg/day)
Trileptal (600 mg/day)
Lithium (1200 mg/day); Celexa (20 mg/day)
Wellbutrin (300 mg/day); Lamotrigine (50 mg/day)
Lithium (900 mg/day); Paroxetine (40 mg/day)
Lamictal (150mg/day); Ativan (0.5mg/day)
Zoloft (150mg/day)
Lamotrigine (50 mg/day)
Lamotrigine (350 mg/day); Bupropion (300 mg/day); Fluoxetine (20 mg/day)
Wellbutrin (200 mg/day)
Venlafaxine (150 mg/day)
Lamictal 300mg/day

Supplemental Table 2. **Correlations among symptoms over time**

The table below presents the Pearson's correlations between Anhedonic Depression subscale of the 62-item Mood and Anxiety Symptom Questionnaire (MASQ-AD), Barratt Impulsiveness Scale (BIS), and Bipolar Inventory of Symptoms Scale - Mania subscale (BISS-mania) for the three time points (baseline, 3-month follow-up (3M), 6-month follow-up (6M)), as well as their correlations with the medication load.

	MASQ-AD baseline	**MASQ-AD 3M**	**MASQ-AD 6M**	**BIS baseline**	**BIS 3M**	**BIS 6M**	**BISS-mania baseline**	**BISS-mania 3M**	**BISS-mania 6M**	**Medication load**
MASQ-AD baseline	1.000	0.697	0.518	0.116	0.259	0.203	-0.192	-0.038	-0.251	-0.154
MASQ-AD 3M	0.697	1.000	0.673	0.030	0.227	0.195	-0.283	-0.126	-0.251	-0.115
MASQ-AD 6M	0.518	0.673	1.000	0.079	0.241	0.345	-0.046	0.069	-0.044	-0.051
BIS baseline	0.116	0.030	0.079	1.000	0.827	0.766	0.196	0.282	0.411	-0.034
BIS 3M	0.259	0.227	0.241	0.827	1.000	0.835	0.206	0.266	0.443	-0.103
BIS 6M	0.203	0.195	0.345	0.766	0.835	1.000	0.151	0.214	0.514	-0.071
BISS-mania baseline	-0.192	-0.283	-0.046	0.196	0.206	0.151	1.000	0.669	0.444	0.000
BISS-mania 3M	-0.038	-0.126	0.069	0.282	0.266	0.214	0.669	1.000	0.268	-0.085
BISS-mania 6M	-0.251	-0.251	-0.044	0.411	0.443	0.514	0.444	0.268	1.000	0.094
Medication load	-0.154	-0.115	-0.051	-0.034	-0.103	-0.071	0.000	-0.085	0.094	1.000

GPM prediction using 10-fold cross-validation

The same procedure was used with a 10-fold cross-validation instead of LOOCV. Since the performance reported from a single k-fold cross-validation run can be noisy, we conducted repeated 10-fold cross-validation with 1000 repetitions. Prediction performance was assessed using the mean MSE across repetitions, and the mean ± standard deviations of the MSE across repetitions are reported below.

- GPM symptom prediction at baseline

At baseline, the GPM predicted anhedonia from the global efficiency of the functional connectome during the RL task [N=61; GPM: MSE=161.29±12.75; null model: MSE=174.03±6.34]. The GPM had a 7.32% lower mean MSE relative to the null model. In addition, the GPM predicted impulsivity from the centrality of the left anterior cingulate cortex (ACC) during resting-state [N=73; GPM: MSE=125.40±7.94; null model: MSE=137.98±4.87]. The GPM had a 9.11% lower mean MSE relative to the null model.

- GPM symptom prediction at 6-month follow-up

At 6-month follow-up, the GPM predicted (hypo)mania from the local efficiency of the left nucleus accumbens (NAc) during the RL task [N=51; GPM: MSE=0.72±0.04; null model: MSE=0.79±0.04]. The GPM had a 9.29% lower MSE relative to the null model. In addition, the GPM predicted anhedonia at 6-month follow-up from the centrality of the left caudate during resting-state [N=64; GPM: MSE=173.09±12.13; null model: MSE=188.97±6.71]. The GPM had an 8.41% lower MSE relative to the null model.

GPM prediction using elastic-net ("GPM elastic-net")

- GPM elastic-net symptom prediction at baseline

At baseline, the GPM elastic-net predicted anhedonia from the RL task functional connectome [GPM elastic-net: MSE=158.46; null model: MSE=176.67]. The GPM elastic-net had a 10.31% lower mean MSE relative to the null model. A hyper-parameter of alpha=0 was chosen, namely, elastic net approached ridge regression and the entire set of graph metrics and baseline symptoms was included in the predictive model. Note that in contrast to the GPM, the GPM elastic-net did not predict impulsivity at baseline.

- GPM elastic-net symptom prediction at 6-month follow-up

The GPM elastic-net predicted anhedonia at 6-month follow-up from the resting-state functional connectome [GPM elastic-net: MSE=168.36; null model: MSE=174.91]. The GPM elastic-net had a 3.74% lower MSE relative to the null model. A hyper-parameter of alpha=1 was chosen indicating that elastic net approached lasso regression with most of the coefficients set to zero (i.e., a small number of variables was used in the predictive model). The centrality of the left caudate, local efficiency of left anterior cingulate cortex, and anhedonia at baseline were included in the predictive model.

The GPM elastic-net predicted impulsivity at 6-month follow-up from the RL task functional connectome [GPM elastic-net: MSE=65.24; null model: MSE=75.40]. The GPM elastic-net had a 13.48% lower MSE relative to the null model. A hyper-parameter of alpha=1 was chosen indicating that elastic net approached lasso regression. The following variables were selected to be included in the predictive model: the clustering coefficient of the left and right caudate, local efficiency of the left nucleus accumbens, centrality of the right anterior cingulate cortex, local efficiency of the right medial orbitofrontal cortex, centrality of the left medial orbitofrontal cortex, as well as anhedonia and impulsivity at baseline. Note that the GPM elastic-net did not predict mania at 6-month follow-up.

Supplemental Figure 1. GPM external validation

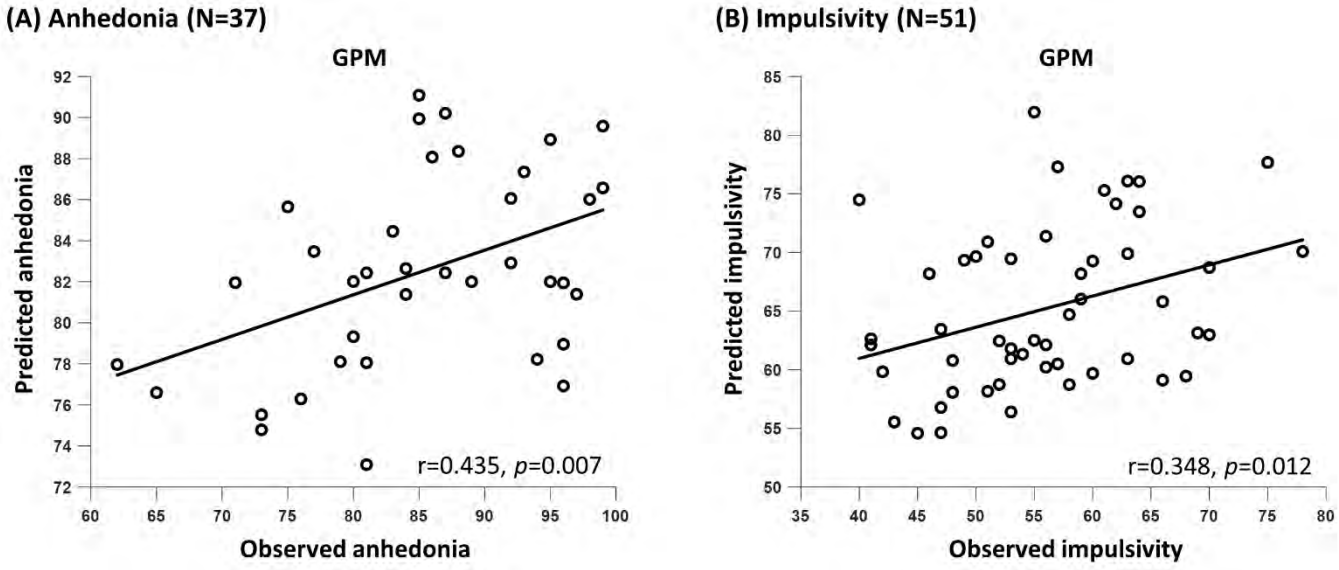

Models were built on the primary sample of individuals with MDD and BP and prediction was done on an external validation sample. The external validation sample comprised individuals with MDD for predicting anhedonia, and a combined sample of individuals with MDD and HC, for predicting impulsivity.

CPM prediction from the positive-only functional connectome

Baseline anhedonia was predicted from the CPM's negative-feature set during the RL task [CPM: r=0.286, p=0.019 permutation testing, MSE=162.60; null model: r=0.070, p=0.161 permutation testing, MSE=172.15]. The CPM had a 5.54% lower MSE relative to the null model. Compared to the GPM, the CPM had a 6.55% higher MSE. Note that these results are similar to the ones obtained with the unthresholded functional connectome (including both positive and negative weights, see Results in the main text).

References

1. Esteban O, Markiewicz CJ, Blair RW, Moodie CA, Isik AI, Erramuzpe A, et al. fMRIPrep: a robust preprocessing pipeline for functional MRI. Nat Methods. 2019;16:111–116.
2. Whitfield-Gabrieli S, Nieto-Castanon A. Conn: a functional connectivity toolbox for correlated and anticorrelated brain networks. Brain Connect. 2012;2:125–141.
3. Behzadi Y, Restom K, Liau J, Liu TT. A component based noise correction method (CompCor) for BOLD and perfusion based fMRI. Neuroimage. 2007;37:90–101.
4. Power JD, Mitra A, Laumann TO, Snyder AZ, Schlaggar BL, Petersen SE. Methods to detect, characterize, and remove motion artifact in resting state fMRI. Neuroimage. 2014;84:320–341.
5. Whitton AE, Kumar P, Treadway MT, Rutherford A V., Ironside ML, Foti D, et al. Mapping Disease Course Across the Mood Disorder Spectrum Through a Research Domain Criteria Framework. Biol Psychiatry Cogn Neurosci Neuroimaging. 2021;6:706–715.
6. Whitton AE, Kumar P, Treadway MT, Rutherford A., Ironside ML, Foti D, et al. Distinct profiles of anhedonia and reward processing and their prospective associations with quality of life among individuals with mood disorders. Mol Psychiatry. 2023:1–19.
7. Rubinov M, Sporns O. Complex network measures of brain connectivity: Uses and interpretations. Neuroimage. 2010;52:1059–1069.
8. Zou H, Hastie T. Regularization and variable selection via the elastic net. J R Stat Soc Ser B Stat Methodol. 2005;67:301–320.
9. Qian J, Hastie T, Friedman J, Tibshirani R, Simon N. Glmnet for Matlab. 2013.
10. Belleau EL, Bolton TAW, Kaiser RH, Clegg R, Cárdenas E, Goer F, et al. Resting state brain dynamics: Associations with childhood sexual abuse and major depressive disorder. NeuroImage Clin. 2022;36:103164.
11. Liu Y, Admon R, Mellem MS, Belleau EL, Kaiser RH, Clegg R, et al. Machine Learning Identifies Large-Scale Reward-Related Activity Modulated by Dopaminergic Enhancement in Major Depression. Biol Psychiatry Cogn Neurosci Neuroimaging. 2020;5:163–172.
12. Knutson B, Westdorp A, Kaiser E, Hommer D. FMRI visualization of brain activity during a monetary incentive delay task. Neuroimage. 2000;12:20–27.
13. Watson D, Clark LA. Mood and Anxiety Symptom Questionnaire. J Behav Ther Exp Psychiatry. 1991.
14. Patton JH, Stanford MS, Barratt ES. Factor structure of the barratt impulsiveness scale. J Clin Psychol. 1995;51:768–774.
15. Pessiglione M, Seymour B, Flandin G, Dolan RJ, Frith CD. Dopamine-dependent prediction errors underpin reward-seeking behaviour in humans. Nature. 2006;442:1042–1045.

16. Shen X, Finn ES, Scheinost D, Rosenberg MD, Chun MM, Papademetris X, et al. Using connectome-based predictive modeling to predict individual behavior from brain connectivity. Nat Protoc. 2017;12:506–518.